Spin-1 Heisenberg chain and the one-dimensional fermion gas

J. Sólyom*
Institut Laue-Langevin, 156X, F-38042 Grenoble CEDEX, France

J. Timonen
Department of Physics, University of Jyväskylä, SF-40100 Jyväskylä, Finland
(Received 10 February 1989; revised manuscript received 22 May 1989)

The composite-spin representation of the spin-1 Heisenberg chain is used to transform it through the Jordan-Wigner transformation to the one-dimensional fermion gas. To properly include the xy couplings between spins, we also consider the bosonized version of the fermion model. Phase diagrams deduced from the two versions of the fermion model are compared against numerical results for finite Heisenberg chains. One of the symmetries of the spin model is lost in the fermionization, and this leads to a topologically incorrect phase diagram in at least one part of the parameter space. There are clear indications of significant coupling of spin and charge degrees of freedom in the fermion model and of strong renormalization of the coupling constants in the continuum limit. The existence of the Haldane gap is discussed in connection with these results.

I. INTRODUCTION

It is well known[1] that in one dimension (1D) fermions can be transformed to bosons and that spin models can be related to either of the two descriptions. These interrelationships between different models have made it possible to predict[2–4] properties of a variety of spin models. Apart from a few special cases the transformations are not exact, however, and there remains the possibility that some properties of the original models are not properly reflected in their transformed counterparts. This could, in particular, be the case when a lattice model has been mapped[2–7] to a field theory. Renormalizations necessary to define the proper continuum limit are not easily handled and the relationships between the parameters of the models are difficult to establish. The true equivalence of the models may be questionable.

It is therefore of interest to study the related 1D models independently and to try to establish whether the predicted equivalence of properties is indeed realized. In this paper we shall do this by comparing the spin-1 Heisenberg chain and the 1D fermion gas model. The spin-1 Heisenberg chain, in a composite spin representation, can be written[5–8] as two coupled spin-$\frac{1}{2}$ chains. Introducing for each of the spin species a Jordan-Wigner transformation to spinless fermions, and then identifying the two kinds of fermions with the two spin components of the same fermion, a mapping to the 1D fermion gas model can be achieved. Apart from the exchange couplings between the transverse components of the two $S=\frac{1}{2}$ operators, the couplings of the spin model can be identified with the interaction terms of the fermion problem. The latter problem has been studied[9] in detail, and a lot of information is available about its phase diagram. We shall compare this phase diagram with the phase diagram of the spin model, which is obtained by extrapolating the finite-chain results.

To study the effect of the exchange couplings between the transverse components of the two $S=\frac{1}{2}$ operators we have used Abelian bosonization[5–7] of fermion operators, even though it is strictly speaking valid only in the scaling limit of small gaps. By combining the boson and fermion results we can then construct the phase diagram of the fermion model which is to be compared with the numerical results. The phase diagram of the fermion model thus constructed will include some of the renormalization effects which are necessary in the continuum limit, and comparison with numerical results will reveal those renormalization effects which are still missing. This comparison will also indicate to what extent the spin and charge degrees of freedom are independent of each other. In a sense this work complements earlier studies[5–7] which were concerned only with the topology of the phase diagrams.

The paper is organized such that in Sec. II we introduce the spin-1 Heisenberg model in the composite spin representation and derive the equivalent fermion model. In Sec. III we derive the bosonized version of the fermion model and in Sec. IV we describe briefly the phase diagrams resulting from these two models. The properties of the original spin-1 model have been calculated numerically for finite chains, and the results of these calculations we describe in Sec. V. Comparison of analytical and numerical results is made in Sec. VI.

II. FERMION REPRESENTATION OF THE SPIN-1 MODEL

The anisotropic Heisenberg chain can be described by the Hamiltonian

$$H=-\sum_{j=1}^{N}[J_{xy}(S_j^xS_{j+1}^x+S_j^yS_{j+1}^y)+J_zS_j^zS_{j+1}^z-D(S_j^z)^2]\ , \tag{2.1}$$

where we have assumed an xy symmetry so that there are only two exchange constants J_{xy} and J_z and a single-ion anisotropy with a characteristic energy D. For spin-1

operators a composite-spin representation can be given in terms of two spin-$\frac{1}{2}$ operators σ_j and τ_j. Replacing $\mathbf{S}_j$ by $\sigma_j+\tau_j$ the Hamiltonian can be written in the form

$$H=H_{\sigma\sigma}+H_{\tau\tau}+H_{\sigma\tau}+H_{\tau\sigma} , \tag{2.2}$$

where

$$H_{\alpha\beta}=-\sum_{j=1}^{N}[\tfrac{1}{2}J_{xy}^{\alpha\beta}(\alpha_j^{+}\beta_{j+1}^{-}+\alpha_j^{-}\beta_{j+1}^{+})+J_z^{\alpha\beta}\alpha_j^z\beta_{j+1}^z -D^{\alpha\beta}\alpha_j^z\beta_j^z] . \tag{2.3}$$

Here we have introduced the usual raising and lowering operators $\alpha^{\pm}=\alpha^x\pm i\alpha^y$ and generalized the coupling constants to allow a departure from (2.1).

It was shown in Ref. 8 that in the case when the couplings $J_{xy}^{\alpha\beta}$, $J_z^{\alpha\beta}$, and $D^{\alpha\beta}$ are independent of the superscripts α and β, the ground-state properties of the composite-spin model are identical to those of the original spin-1 model with couplings J_{xy}, J_z, and D, at least for small D. The additional local singlets due to the composite-spin representation will lead to extra levels which are, however, separated from the ground state by an energy which is proportional to the largest of the parameters J_{xy} and J_z.

As in Ref. 8 we shall now simplify the model by assuming that there are only six different coupling constants such that

$$H_{\sigma\sigma}=-\sum_{j=1}^{N}[\tfrac{1}{2}J_{xy}(\sigma_j^{+}\sigma_{j+1}^{-}+\sigma_j^{-}\sigma_{j+1}^{+})+J_z\sigma_j^z\sigma_{j+1}^z -D(\sigma_j^z)]$$

and (2.4)

$$H_{\sigma\tau}=-\sum_{j=1}^{N}[\tfrac{1}{2}J'_{xy}(\sigma_j^{+}\tau_{j+1}^{-}+\sigma_j^{-}\tau_{j+1}^{+})+J'_z\sigma_j^z\tau_{j+1}^z -D'\sigma_j^z\tau_j^z] .$$

$H_{\tau\tau}$ and $H_{\tau\sigma}$ can be found from these expressions by interchanging all the σ and τ operators. The last term in $H_{\sigma\sigma}$ (and $H_{\tau\tau}$) is constant when $\sigma=\tau=\frac{1}{2}$, and we shall fix the energy scale by choosing $J_{xy}=1$. We are therefore left with four independent coupling constants, J'_{xy}, J_z, J'_z and D'.

$H_{\sigma\sigma}$ and $H_{\tau\tau}$ correspond to independent spin-$\frac{1}{2}$ Heisenberg chains, while $H_{\sigma\tau}$ and $H_{\tau\sigma}$ describe the coupling between them. Next we shall make a Jordan-Wigner transformation to fermions. For a single spin-$\frac{1}{2}$ chain the transformation is to spinless fermions. In our case[10] the σ spins can be transformed to up-spin fermions and the τ spins to down-spin fermions. The correct commutation relations are satisfied if we choose

$$\begin{aligned}
\sigma_j^{+}&=c_{j\uparrow}^{\dagger}\exp\left[i\pi\sum_{n=1}^{j-1}c_{n\uparrow}^{\dagger}c_{n\uparrow}\right] ,\\
\sigma_j^{-}&=\exp\left[-i\pi\sum_{n=1}^{j-1}c_{n\uparrow}^{\dagger}c_{n\uparrow}\right]c_{j\uparrow} ,\\
\sigma_j^z&=c_{j\uparrow}^{\dagger}c_{j\uparrow}-\tfrac{1}{2} ,\\
\tau_j^{+}&=c_{j\downarrow}^{\dagger}\exp\left[i\pi\sum_{n=1}^{j-1}c_{n\downarrow}^{\dagger}c_{n\downarrow}+i\pi\sum_{n=1}^{N}c_{n\uparrow}^{\dagger}c_{n\uparrow}\right] ,\\
\tau_j^{-}&=\exp\left[-i\pi\sum_{n=1}^{j-1}c_{n\downarrow}^{\dagger}c_{n\downarrow}-i\pi\sum_{n=1}^{N}c_{n\uparrow}^{\dagger}c_{n\uparrow}\right]c_{j\downarrow} ,\\
\tau_j^z&=c_{j\downarrow}^{\dagger}c_{j\downarrow}-\tfrac{1}{2} ,
\end{aligned} \tag{2.5}$$

where $c_{j\sigma}^{\dagger}$ and $c_{j\sigma}$ are the usual fermion creation and annihilation operators.

In terms of these operators $H_{\sigma\sigma}$ and $H_{\tau\tau}$ can be written in a simple form,

$$H_{\sigma\sigma}+H_{\tau\tau}=-\sum_{j=1,\sigma}^{N}\tfrac{1}{2}(c_{j\sigma}^{\dagger}c_{j+1,\sigma}+c_{j+1,\sigma}^{\dagger}c_{j\sigma}) -J_z\sum_{j=1,\sigma}^{N}(c_{j\sigma}^{\dagger}c_{j\sigma}-\tfrac{1}{2})(c_{j+1,\sigma}^{\dagger}c_{j+1,\sigma}-\tfrac{1}{2}) , \tag{2.6}$$

where a constant proportional to D has been dropped. The first term describes the hopping of electrons, while the second term is a Coulomb coupling between electrons on neighboring sites.

Using the same transformation for $h_{\sigma\tau}$ and $h_{\tau\sigma}$, the transverse exchange would lead to a hopping term with spin flip and a complicated phase factor. We shall neglect this term first and consider only the longitudinal part. The transformed Hamiltonian in terms of fermions then takes the form

$$\begin{aligned}
H_{\sigma\tau}^z+H_{\tau\sigma}^z&=-J'_z\sum_{j=1,\sigma}^{N}(c_{j\sigma}^{\dagger}c_{j\sigma}-\tfrac{1}{2})(c_{j+1,-\sigma}^{\dagger}c_{j+1,-\sigma}-\tfrac{1}{2})\\
&\quad+D'\sum_{j=1,\sigma}^{N}(c_{j\sigma}^{\dagger}c_{j\sigma}-\tfrac{1}{2})(c_{j,-\sigma}^{\dagger}c_{j,-\sigma}-\tfrac{1}{2}) .
\end{aligned} \tag{2.7}$$

The fermion model is usually given in the momentum representation. The first term in (2.6) is the free-particle contribution with a $\cos(ka)$ spectrum. We assume that the ground state is nonmagnetic with $\langle\sigma_j^z\rangle=\langle\tau_j^z\rangle=0$, which corresponds to a half-filled band. Linearizing the spectrum around the two Fermi points $\pm k_F=\pm\pi/2a$, and assuming that in the interaction terms the important processes are those where all the participating fermions are close to one of the Fermi points, the Hamiltonian $H_{\sigma\sigma}+H_{\tau\tau}+H_{\sigma\tau}^z+H_{\tau\sigma}^z$ takes the form of a general interacting 1D fermion problem[9] with backward, forward, and umklapp scattering terms. Using the notations of the

"g-ology" model, the couplings can be identified as

$$\frac{g_{1\parallel}}{v_F}=4J_z-2(J_z'-D'),\quad \frac{g_{1\perp}}{v_F}=2(J_z'+D'),$$
$$\frac{g_{2\parallel}}{v_F}=\frac{g_{2\perp}}{v_F}=-2(J_z'-D'),\quad \frac{g_3}{v_F}=2(J_z'+D'),$$
$$\frac{g_{4\parallel}}{v_F}=-4J_z,\quad \frac{g_{4\perp}}{v_F}=-2(J_z'-D'). \tag{2.8}$$

As pointed out by Fowler[11] and Schulz,[7] the derivation of $g_{4\parallel}$ needs special care. The Hartree-Fock corrections to the self-energy have to be analyzed carefully. In the special case when $J_z'=J_z$, the model is equivalent to the half-filled extended Hubbard model with $U=2D$ and $V=-J_z$ as the on-site and intersite Coulomb couplings, respectively. In this case the equivalence is valid also for the lattice version of the model, and not only in the continuum limit.

III. BOSON REPRESENTATION

As mentioned above, the coupling J_{xy}' between the two spin species cannot be given in a simple form in the fermion language. We shall try to estimate its effect with the help of the bosonized version of the fermion model. The bosonization rules are well documented,[5,6,7,9,12] but since different authors use a somewhat different notation, we give our version here.

The fermion density operators

$$\rho_\sigma(p)=\sum_k c_{k+p,\sigma}^\dagger c_{k\sigma} \tag{3.1}$$

are separated for small momentum p into two contributions, coming from the neighborhood of the $+k_F$ and $-k_F$ Fermi points,

$$\rho_\sigma(p)=\rho_{+,\sigma}(p)+\rho_{-,\sigma}(p). \tag{3.2}$$

The charge and spin density operators are defined for the right-going and left-going fermions as

$$\rho_\pm(p)=\frac{1}{\sqrt{2}}[\rho_{\pm,\uparrow}(p)+\rho_{\pm,\downarrow}(p)],$$
$$\sigma_\pm(p)=\frac{1}{\sqrt{2}}[\rho_{\pm,\uparrow}(p)-\rho_{\pm,\downarrow}(p)]. \tag{3.3}$$

Boson phase fields are then introduced by

$$\phi_\rho(x)=\frac{-i}{\sqrt{4\pi}}\frac{2\pi}{L}\sum_p \frac{\exp\left[-\frac{\alpha}{2}|p|-ipx\right]}{p}\times[\rho_+(p)+\rho_-(p)],$$
$$\pi_\rho(x)=\frac{1}{\sqrt{4\pi}}\frac{2\pi}{L}\sum_p \exp\left[-\frac{\alpha}{2}|p|-ipx\right]\times[\rho_+(p)-\rho_-(p)],$$
$$\phi_\sigma(x)=\frac{-i}{\sqrt{4\pi}}\frac{2\pi}{L}\sum_p \frac{\exp\left[-\frac{\alpha}{2}|p|-ipx\right]}{p}\times[\sigma_+(p)+\sigma_-(p)], \tag{3.4}$$
$$\pi_\sigma(x)=\frac{1}{\sqrt{4\pi}}\frac{2\pi}{L}\sum_p \exp\left[-\frac{\alpha}{2}|p|-ipx\right]\times[\sigma_+(p)-\sigma_-(p)],$$

where α is a cutoff parameter. The field variables ϕ_ρ and ϕ_σ and the related canonical momenta π_ρ and π_σ satisfy canonical commutation relations. To express the fermion operators in terms of the phase fields, two extra variables, χ_ρ and χ_σ, are needed,

$$\chi_\rho(x)=\frac{-i}{\sqrt{4\pi}}\frac{2\pi}{L}\sum_p \frac{\exp\left[-\frac{\alpha}{2}|p|-ipx\right]}{p}\times[\rho_+(p)-\rho_-(p)],$$
$$\chi_\sigma(x)=\frac{-i}{\sqrt{4\pi}}\frac{2\pi}{L}\sum_p \frac{\exp\left[-\frac{a}{2}|p|-ipx\right]}{p}\times[\sigma_+(p)-\sigma_-(p)]. \tag{3.5}$$

These variables satisfy

$$\pi_\rho(x)=\frac{\partial\chi_\rho(x)}{\partial x},\quad \pi_\sigma(x)=-\frac{\partial\chi_\sigma(x)}{\partial x}. \tag{3.6}$$

With these definitions the g-ology model of 1D fermions[9] can be written as

$$H=H_c+H_s, \tag{3.7}$$

with

$$H_c=\int dx\,\tfrac{1}{2}\left[A_\rho\pi_\rho^2(x)+B_\rho\left[\frac{\partial\phi_\rho(x)}{\partial x}\right]^2\right]+C_\rho\int dx\,\cos[\sqrt{8\pi}\phi_\rho(x)] \tag{3.8}$$

and

$$H_s=\int dx\,\tfrac{1}{2}\left[A_\sigma\pi_\sigma^2(x)+B_\sigma\left[\frac{\partial\phi_\sigma(x)}{\partial x}\right]^2\right]+C_\sigma\int dx\,\cos[\sqrt{8\pi}\phi_\sigma(x)], \tag{3.9}$$

where

$$A_\rho=v_F\left[1-\frac{1}{2\pi v_F}(2g_2-g_{1\parallel}-g_{4\parallel}-g_{4\perp})\right],$$
$$B_\rho=v_F\left[1+\frac{1}{2\pi v_F}(2g_2-g_{1\parallel}+g_{4\parallel}+g_{4\perp})\right],$$
$$C_\rho=\frac{2}{(2\pi\alpha)^2}g_3,$$
$$A_\sigma=v_F\left[1+\frac{1}{2\pi v_F}(g_{1\parallel}+g_{4\parallel}-g_{4\perp})\right], \tag{3.10}$$
$$B_\sigma=v_F\left[1-\frac{1}{2\pi v_F}(g_{1\parallel}-g_{4\parallel}+g_{4\perp})\right],$$
$$C_\sigma=\frac{2}{(2\pi\alpha)^2}g_{1\perp}.$$

The velocities of the charge- and spin-density modes are

$$u_\rho = v_F \left[\left[1+\frac{1}{2\pi v_F}(g_{4\parallel}+g_{4\perp}) \right]^2 - \left[\frac{1}{2\pi v_F}(2g_2-g_{1\parallel}) \right]^2 \right]^{1/2},$$
$$u_\sigma = v_F \left[\left[1+\frac{1}{2\pi v_F}(g_{4\parallel}-g_{4\perp}) \right]^2 - \left[\frac{1}{2\pi v_F} g_{1\parallel} \right]^2 \right]^{1/2}. \tag{3.11}$$

Inserting from Eq. (2.8) the spin-coupling equivalents of the g-ology couplings we find for the velocities of the two modes

$$u_\rho = v_F \left[1-\frac{2}{\pi}(2J_z+J_z'-D') \right]^{1/2},$$
$$u_\sigma = v_F \left[1-\frac{2}{\pi}(2J_z-J_z'+D') \right]^{1/2}, \tag{3.12}$$

while

$$C_\sigma = C_\rho \sim J_z'+D' . \tag{3.13}$$

These results are straightforward generalizations of those obtained by Schulz.[7]

The bosonized Hamiltonian presented above is the equivalent of the g-ology model. In that model there are no umklapp processes between fermions of identical spin if the interaction is local. In the spin model the interaction is between neighboring sites, and as shown by den Nijs,[5] a careful analysis will lead to umklapp processes even for spinless fermions. Using the same arguments, the longitudinal parts of $H_{\sigma\sigma}$ and $H_{\tau\tau}$ will lead to an additional term H_{umklapp} in the Hamiltonian which will couple the charge- and spin-density degrees of freedom,

$$H_{\text{umklapp}} = -\frac{J_z}{(\pi\alpha)^2}\int dx \cos(\sqrt{8\pi}\phi_\rho)\cos(\sqrt{8\pi}\phi_\sigma) . \tag{3.14}$$

The numerical results will indicate how important this coupling is. Note, however, that there may be other sources for the coupling between charge degrees and spin degrees of freedom, e.g., the finite bandwidth of the fermion model. These effects will not be analyzed here.

We still have to consider the transverse part of the coupling between the two spin species,

$$H_{\text{tr}} = H_{\sigma\tau}^{xy} + H_{\tau\sigma}^{xy} = -J_{xy}'\sum_j (\sigma_j^+\tau_{j+1}^- + \sigma_j^-\tau_{j+1}^+ + \tau_j^+\sigma_{j+1}^- + \tau_j^-\sigma_{j+1}^+) . \tag{3.15}$$

As shown by Schulz,[7] in boson variables this operator takes the form

$$H_{\text{tr}} = -\frac{J_{xy}'}{(\pi\alpha)^2}\int dx \cos(\sqrt{2\pi}\chi_\sigma) . \tag{3.16}$$

Collecting all the terms, the bosonized version of the spin-1 composite spin Hamiltonian becomes

$$H = H_\rho + H_\sigma + H_{\text{umklapp}} \tag{3.17}$$

with

$$H_\rho = \int dx \left\{ \frac{1}{2}\left[\pi_\rho^2(x) + u_\rho^2 \left[\frac{\partial\phi_\rho(x)}{\partial x} \right]^2 \right] + \frac{J_z'+D'}{(\pi\alpha)^2}\cos(\sqrt{8\pi}\phi_\rho) \right\},$$
$$H_\sigma = \int dx \left\{ \frac{1}{2}\left[\pi_\sigma^2(x) + u_\sigma^2 \left[\frac{\partial\phi_\sigma(x)}{\partial x} \right]^2 \right] + \frac{J_z'+D'}{(\pi\alpha)^2}\cos(\sqrt{8\pi}\phi_\sigma) - \frac{J_{xy}'}{(\pi\alpha)^2}\cos(\sqrt{2\pi}\chi_\sigma) \right\}, \tag{3.18}$$

where u_ρ and u_σ are given by (3.12) and H_{umklapp} is given by (3.14).

In comparison with earlier work we have derived the bosonized Hamiltonian for a more general choice of couplings. We have also shown explicitly that, due to umklapp processes, there is a coupling between the charge-density and spin-density sectors. Its effect is difficult to estimate analytically. In Sec. IV we shall analyze the model without H_{umklapp}.

IV. PHASE DIAGRAM OF THE FERMION MODEL

The 1D fermion model has been analyzed[9] in detail in various approximations. The bosonized form of it separates into charge-density and spin-density degrees of freedom: the charge-density part depends on couplings $g_{1\parallel}-2g_2$ and g_3, while the spin-density part depends on $g_{1\parallel}$ and $g_{1\perp}$. This separation is found[9] also in the scaling equations for these couplings.

It is known from the scaling equations that the umklapp processes are irrelevant and the charge-density excitations are gapless if

$$|g_3| \le g_{1\parallel}-2g_2 . \tag{4.1}$$

Similarly, the backward scattering processes are irrelevant and the spin-density excitations are gapless if

$$|g_{1\perp}| \le g_{1\parallel} . \tag{4.2}$$

Otherwise in either one or both sectors a gap appears.

The stability of the fermion model poses additional conditions on the couplings. These conditions are most easily found in the bosonized version of the model. Velocities u_ρ and u_σ both have to be positive, i.e.,

$$\frac{1}{2\pi v_F}|g_{1\parallel}-2g_2| \le 1+\frac{1}{2\pi v_F}(g_{4\parallel}+g_{4\perp}),$$
$$\frac{1}{2\pi v_F}|g_{1\parallel}| \le 1+\frac{1}{2\pi v_F}(g_{4\parallel}-g_{4\perp}) \tag{4.3}$$

must be satisfied for the continuum limit model to be valid.

Transformation of the g couplings to the couplings of the spin model is given by (2.8), and through these relations the phase and stability boundaries can be transformed to the corresponding boundaries in the spin-1 model. Equations (4.3) mean that the continuum limit description is valid if

$$4J_z+2(J_z'-D')\leq\pi,\quad 4J_z-2(J_z'-D')\leq\pi\ . \tag{4.4}$$

In the spin language these boundaries correspond to transitions to a new type of order, e.g., ferromagnetic ordering.

Provided that the conditions (4.4) are satisfied, ϕ_ρ in the H_ρ of (3.18) is a free massless field if $J_z'+D'=0$. Otherwise a gap is generated by the operator $\cos(\sqrt{8\pi}\phi_\rho)$, if, furthermore,

$$4J_z+2(J_z'-D')<2|J_z'+D'|\ . \tag{4.5}$$

H_σ given in Eq. (3.18) contains two operators which can be relevant, $\cos(\sqrt{8\pi}\phi_\sigma)$, with a coefficient proportional to $(J_z'+D')$, and $\cos(\sqrt{2\pi}\chi_\sigma)$, with a coefficient proportional to J_{xy}'. Considering first the case when $J_{xy}'=0$, H_σ describes then a free massless field for $J_z'=D'=0$. Otherwise the operator $\cos(\sqrt{8\pi}\phi_\sigma)$ will generate a gap if in addition

$$4J_z-3(J_z'-D')<2|J_z'+D'| \tag{4.6}$$

is satisfied.

We show in Figs. 1 and 2 the phase diagram of the spin model in two special cases, namely, for $J_z'=J_z$ and for $D'=0$. The phases of these diagrams are characterized by vanishing or finite values of the charge-density gap Δ_ρ and the spin-density gap Δ_σ. In both cases the lines where u_ρ or u_σ vanishes separate a phase in which

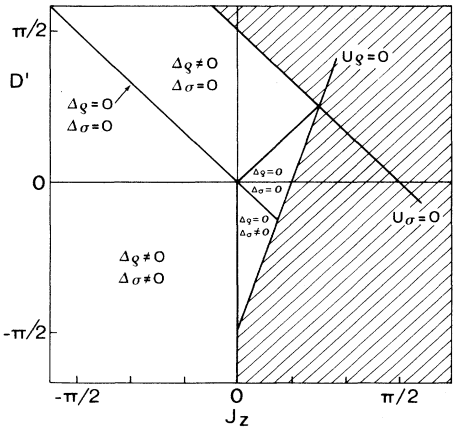

FIG. 1. Phase diagram of the fermion model in the J_zD' plane for $J_{xy}'=0$ and $J_z=J_z'$. In the shaded region the model is unstable. The different phases are characterized by vanishing or finite values of the charge-excitation and spin-excitation gaps, Δ_ρ and Δ_σ, respectively.

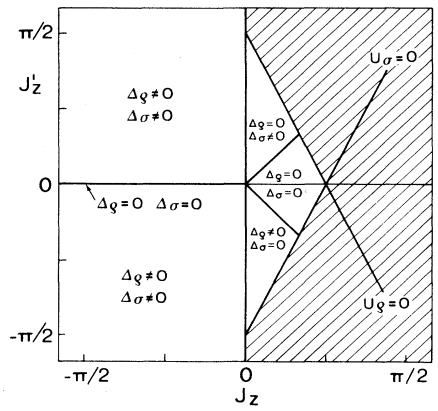

FIG. 2. Phase diagram of the fermion model in the J_zJ_z' plane for $J_{xy}'=0$ and $D'=0$.

$\langle\sigma_j^z\rangle=\langle\tau_j^z\rangle=0$ from a phase in which this does not hold. To the right of the line $u_\rho=0$, a ferromagnetic phase appears with $\langle\sigma_i^z\rangle+\langle\tau_i^z\rangle\neq0$, while to the right of the line $u_\sigma=0$, $\langle\sigma_i^z\rangle+\langle\tau_i^z\rangle=0$ but $\langle\sigma_i^z\rangle-\langle\tau_i^z\rangle\neq0$. The first case corresponds to a ferromagnetic phase, while the second phase is a so-called impurity phase. The ground state of the impurity phase is a singlet which is formed of the local impurity singlet states arising from the two spin-$\frac{1}{2}$ operators.

In both of the Figs. 1 and 2 there are three gapless regions. In one of these three regions Δ_ρ and Δ_σ both vanish, in one of them Δ_ρ is finite, and in one of them Δ_σ is finite. There is also a massive region where both gaps are finite.

To see the difference between the phases corresponding to these various regions, one can analyze three correlation functions as discussed by Schulz.[7] These are

$$\begin{aligned}&G_\perp(x,t)=\langle S^+(x,t)S^-(0,0)\rangle\ ,\\ &G_{\perp2}(x,t)=\langle[S^+(x,t)]^2[S^-(0,0)]^2\rangle\ ,\\ &G_z(x,t)=\langle S^z(x,t)S^z(0,0)\rangle\ .\end{aligned} \tag{4.7}$$

Using the composite-spin representation, the Jordan-Wigner transformation, and the bosonization rules, these correlation functions can be expressed in terms of boson phase variables and can be evaluated. Depending on whether the charge-density or spin-density excitations have vanishing or finite gap, an algebraic or an exponential decay of correlations will be found. Without going into details, the general behavior of the correlation functions indicates that in our calculations of the energy gaps of finite systems, three kinds of excitations have to be considered: (i) excitations with one spin flip (S^+), (ii) excitations with two spin flips [$(S^+)^2$], and (iii) excitations without a spin flip (S^z).

Note that the model discussed until now, i.e., $J_{xy}'=0$, corresponds to the extended Hubbard model with on-site and intersite Coulomb couplings, where

$$U=2D',\quad V=-J_z=-J_z'\ , \tag{4.8}$$

respectively. The region where Δ_ρ and Δ_σ both are finite corresponds to the charge-density-wave (CDW) phase. The region where Δ_ρ is finite but Δ_σ vanishes corresponds to the spin-density-wave (SDW) phase. The region where Δ_σ is finite but Δ_ρ vanishes corresponds to the singlet pairing (SP) superconductivity, while the region where both gaps vanish is that of the triplet pairing (TP) superconductivity. The boundary between the CDW and SP phases ($V=0$ and $U<0$) is known to be exact, while the other boundaries ($U=\pm 2V$) are only approximate.[13]

We now turn to the case when $J'_{xy}\neq 0$. In the H_σ of (3.18) there are now two possibly relevant operators. As was shown by den Nijs,[5] this model has the symmetry of an Ising model and one of the two operators is always relevant. The scaling dimensions of the two operators $\cos(\sqrt{8\pi}\phi_\sigma)$ and $\cos(\sqrt{2\pi}\chi_\sigma)$ become equal at

$$\left[\frac{u_\sigma}{v_F}\right]^2 = 1-\frac{2}{\pi}(2J_z-J'_z+D')=4 \ . \tag{4.9}$$

For small values of $2J_z-J'_z+D'$ the dominant perturbation is $\cos(\sqrt{2\pi}\chi_\sigma)$ which produces a gap for the spin-density excitations. An ordered state can appear only for large negative values of $2J_z-J'_z+D'$.

The phase diagram for an arbitrary finite J'_{xy} is given in Figs. 3 and 4 for the cases $J'_z=J_z$ and $D'=0$, respectively. As noted before, the effects of the J'_{xy} coupling cannot be analyzed in the fermion model, and we have to use the bosonized version of the model to estimate these effects. As the spin-density sector of the model is always massive, it is the charge-density sector which will determine the phase boundaries. In those parts of the phase diagram of the bosonized model which are not affected by the J'_{xy} coupling, we will still use the fermion results described above. The extra phase boundaries induced by the J'_{xy} coupling are accepted in their bosonized form and, therefore, will not include any renormalization effects. Using the same arguments as before it follows that an extended region with a singlet ground state will appear already for small J'_{xy}. As J'_{xy} increases the boundary of the ordered phase is perhaps renormalized, but as J'_{xy} goes to zero, the width of the singlet region should not vanish.

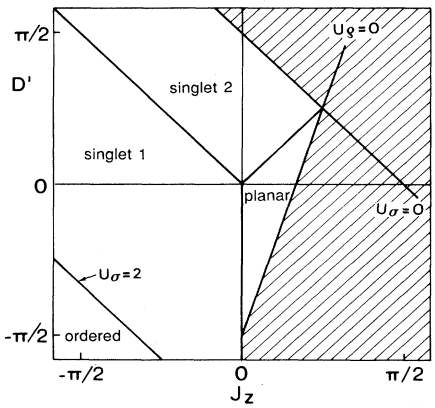

FIG. 3. Phase diagram of the fermion model in the J_zD' plane for $J'_{xy}\neq 0$ and $J_z=J'_z$. The boundary of the ordered phase is shifted upwards to be seen in the figure.

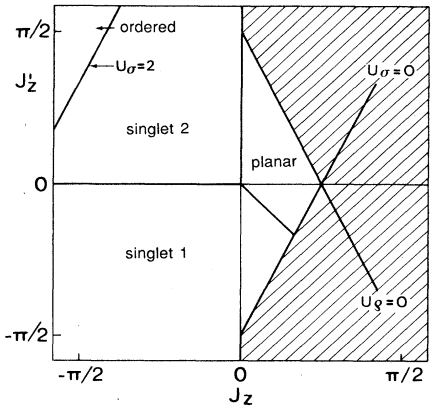

FIG. 4. Phase diagram of the fermion model in the $J_zJ'_z$ plane for $J'_{xy}\neq 0$ and $D'=0$. The boundary of the ordered phase is shifted downwards to be seen in the figure.

The phase diagram of Fig. 3 differs from that given by Schulz[7] in the extents of the planar phases. This difference arises from the fact he did not take into account the renormalization of the couplings when determining the phase boundaries which are not affected by the J'_{xy} coupling, while we used conditions (4.1) and (4.2) which result from a renormalization-group calculation. The second planar phase of Schulz is also missing in our phase diagram. It results from two-spin-flip processes and shows up only in the secondary gap. Therefore it appears in our numerical results, but not in the fermion model results where primary gap is the relevant quantity. The difference between the two planar phases can be found in the bosonized version of the model by looking at the asymptotic behavior of correlation functions.[7] In the present analysis we resort to the bosonization results only when the fermion model cannot be used and, therefore, we have left out the second planar phase in Fig. 3.

Until now the umklapp processes described by H_{umklapp} in (3.14) have been completely neglected. This operator which couples the charge-density and spin-density excitations may modify the picture considerably. A consequence of this coupling is that the boundary of the ferromagnetic phase, which is determined by $u_\rho=0$, can be renormalized by the J'_{xy} terms even though these terms appear only in the spin-density sector described by H_σ. The boundaries of the other phases can be shifted as well. Analytic evaluation of the effects of this coupling is difficult, but our numerical results described in Sec. V will indicate the importance of this coupling even though we will not analyze its effect separately.

V. NUMERICAL RESULTS FOR THE SPIN-1 MODEL

In this section we describe our numerical studies of the Hamiltonian (2.2). The ground-state and low-lying excitations are calculated by exact diagonalization of the

Hamiltonian for finite chains containing $N < 10$ sites with periodic boundary conditions. The states of the system can be classified by their momentum k by the z component of their total spin $S^z_{\rm tot}$ and by their symmetry under interchange of the σ_j and τ_j spins.

The ground state of a finite chain is either in the $S^z_{\rm tot}=0$ or in the $S^z_{\rm tot}=\pm N$ subspace. The latter state is an aligned ferromagnetic state. The stability region of the ferromagnetic phase can be easily obtained from the crossover between the two subspaces. The lines along which the lowest energies of the $S^z_{\rm tot}=0$ and $S^z_{\rm tot}=\pm N$ subspaces are equal converge very rapidly towards their infinite chain length positions. In the parameter range where the ground state is an $S^z_{\rm tot}=0$ state, the ground-state wave function is translationally invariant ($k=0$) and is symmetric under the interchange of σ_j and τ_j.

The first excited state above this ground state will have different quantum numbers in different regions of the phase space. It can, e.g., be a state with zero, one or two spin flips, having thus $S^z_{\rm tot}=0$, ± 1, or ± 2. In the first case the wave function either has momentum $k=\pi$ or is antisymmetric under the interchange of σ_j and τ_j, or both happen.

For a finite system the first excited state is separated from the ground state by a finite gap. If in the thermodynamic limit this gap remains finite, the ground state is a singlet. Otherwise, if the gap vanishes exponentially fast as the system size increases, an ordered phase develops. If the vanishing of the gap is given by a power law, a state with critical behavior is found.

We shall use below the following notation. ΔE^s_{00} is the energy difference between the ground state and the lowest excited state in the sector $S^z_{\rm tot}=0$ which is symmetric with respect to σ_j and τ_j. ΔE^a_{00} is the energy difference between the ground state and the lowest excited state in the sector $S^z_{\rm tot}=0$ which is antisymmetric with respect to the interchange of σ_j and τ_j. ΔE_{01} is the gap to the lowest-lying state in the $S^z_{\rm tot}=\pm 1$ sector and ΔE_{02} is the gap to the lowest-lying state in the $S^z_{\rm tot}=\pm 2$ sector.

As a study case we will first consider Hamiltonian (2.2) with $J'_z=J_z$ and explore its phase diagram in the J_zD' phase. At $J'_{xy}=0$ the model is equivalent to the extended Hubbard model, as mentioned above, and the phase diagram of this model has been studied by various methods[13–15] including finite-chain calculations. From our numerical results for the stability of the ferromagnetic phase, and for the chain length dependence of the various gaps, we find the phase diagram shown in Fig. 5. It shows a considerable similarity with the phase diagram of Fig. 1 obtained in the continuum limit.

In addition to the ferromagnetic phase there are four other phases. In the antiferromagnetic phase the gap ΔE^s_{00} vanishes exponentially fast with the chain length leading thus to an ordered state. In the planar 1 phase the spin-flip gaps vanish proportionally to the inverse chain lengths. In the planar 2 phase ΔE_{01} remains finite, but ΔE_{02} will vanish for infinite chains. Finally, in the phase denoted as impurity planar phase ΔE^a_{00} vanishes as $1/N$. The antisymmetric combination of σ_j and τ_j gives a local singlet which should not be present in a true spin-1 model, hence the name impurity phase.

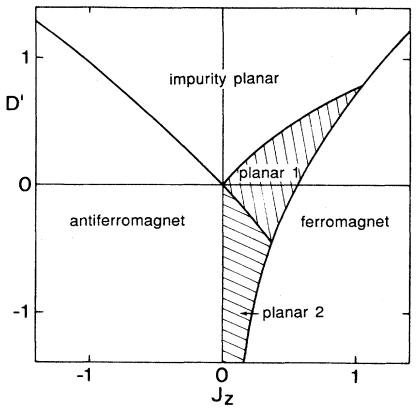

FIG. 5. Phase diagram of the composite-spin model in the J_zD' plane for $J'_{xy}=0$ and $J_z=J'_z$.

Apart from the ferromagnetic phase where convergence is fast, the phase boundaries cannot be determined with high precision from a finite-size calculation. As an illustration we show in Fig. 6 the scaled mass gap ratios $(N+2)\Delta E(N+2)/N\Delta E(N)$ for $J_z=J'_z=-0.5$ and for varying D'. The solid line is the ratio for the ΔE_{01} gap, the dashed line is that for the ΔE^s_{00} gap, while the ratio for the ΔE^a_{00} gap is shown as a dashed-dotted line. The phase boundaries are determined by the condition that the scaled mass gap ratio is unity. From the available nu-

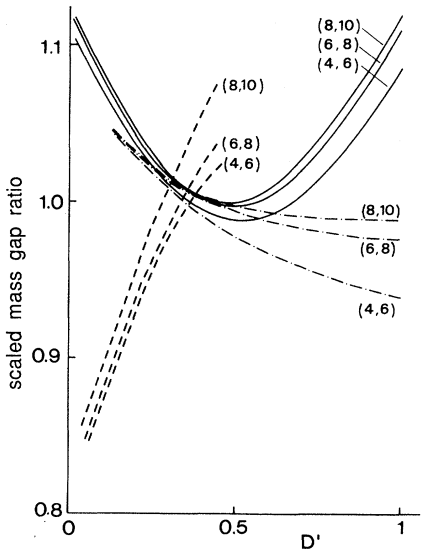

FIG. 6. Scaled mass gap ratios for the gaps ΔE_{01} (solid lines), ΔE^s_{00} (dashed lines), and ΔE^a_{00} (dashed-dotted lines) vs D' for $J_z=J'_z=-0.5$ and $J'_{xy}=0$, comparing chains with $N=4$, 6, and 8 sites to chains with $N+2=6$, 8, and 10 sites.

merical results the transition from the antiferromagnetic phase to the planar impurity phase cannot be located precisely. It can be deduced, however, that for $J_z=J_z'=-0.5$ this transition is close to $D'=0.5$, and that the spin-flip gap vanishes at the transition point. For large negative values of J_z, where the phase transition in the extended Hubbard model is known to be of first order, this softening of the spin-flip excitations will not happen. On the other hand, for $J_z>0$ the spin-flip excitations are soft over an extended range of D as shown in Fig. 7 for $J_z=J_z'=0.2$. It is also seen in this figure that the two-spin-flip excitations are soft over a larger range than the one-spin-flip excitations, thus giving rise to the planar 2 phase.

When the J_{xy}' term is introduced as a perturbation, a phase diagram like the one shown in Fig. 3 should be obtained. On both sides of the line $J_z+D'=0$ a singlet ground state should be found, and the ordered antiferromagnetic phase should be pushed further towards negative J_z, while the boundary of the ferromagnetic phase should remain unchanged.

The numerical results do not quite agree with the expectations. The discrepancy could, however, be explained as a renormalization of the coupling constants. The ferromagnetic phase boundary is shifted as J_{xy}' increases, indicating that J_{xy}', which acts in the spin-density sector, affects also the charge-density sector. This means that there is a coupling of charge and spin degrees of freedom, probably through the umklapp processes which have been neglected until now. The impurity planar phase disappears as expected, and above the line $D'+J_z=0$ all excitations acquire a gap. The boundary of the antiferromagnetic phase is also shifted, although proportionally to J_{xy}', which is in contrast with the continuum limit result. We show in Fig. 8 the phase diagram estimated from finite-size scaling for $J_{xy}'=0.2$. To illustrate the difficulties in determining the phase boundaries we show in Fig. 9 the scaled mass gap ratios for $J_z=J_z'=-0.5$. Comparison with Fig. 6, which shows the scaled mass gap ratios for the same J_z but for $J_{xy}'=0$, indicates clearly that for a finite J_{xy}' the gap ΔE_{00}^a is finite for $D'>-J_z$. Similarly ΔE_{00}^s increases with J_{xy}' and therefore in an infinite chain this gap becomes finite at a smaller value of D' than ΔE_{00}^a. On the other hand ΔE_{01} decreases when J_{xy}' is introduced. From numerical results alone one cannot say for sure that the spin-flip gap vanishes at only a single value of D', which would result in a line between the two singlet phases where the gap vanishes. Nevertheless, we have assumed this to be true in drawing Fig. 8 to be consistent with the continuum-limit results.

When $J_{xy}'=1$ the model is equivalent to the spin-1 Heisenberg model with single-ion anisotropy, and the

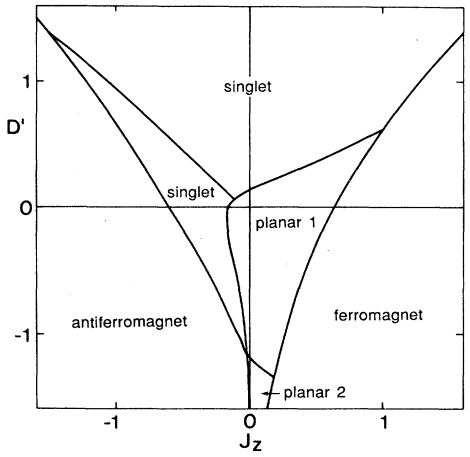

FIG. 8. Phase diagram of the composite-spin model in the J_zD' plane for $J_z=J_z'$ and $J_{xy}'=0.2$.

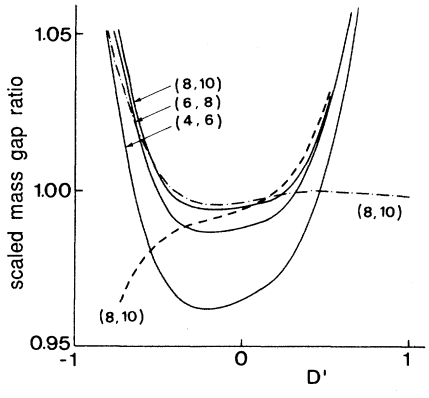

FIG. 7. Scaled mass gap ratios for the gaps ΔE_{01} (solid lines), ΔE_{02} (dotted lines) and ΔE_{00}^a (dashed-dotted lines) vs D' for $J_z=J_z'=0.2$ and $J_{zy}'=0$. For ΔE_{02} and ΔE_{00}^a the comparison is shown only for $N=8$ and $N=10$.

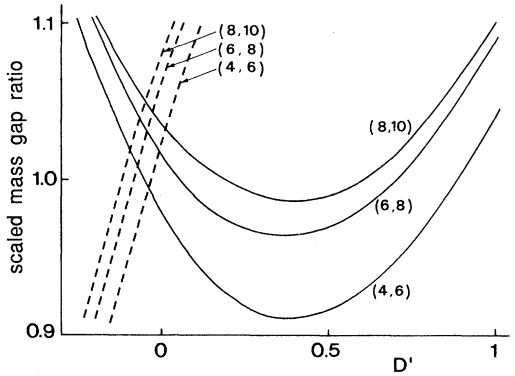

FIG. 9. Same as Fig. 6 but for $J_{xy}'=0.2$. The scaled mass gap ratios for ΔE_{00}^s are not shown since they are much larger than unity.

phase diagram given by Botet *et al.*[16] and by Schulz and Ziman[17] has to be recovered. The spin-1 phase diagram differs from Fig. 8 only in the positions of the transition lines; the topologies of the phase diagrams are the same. To have a clear picture of the kind of numerical evidence on which the spin-1 phase diagram is based, we show in Fig. 10 the scaled mass gap ratios of ΔE_{01} and ΔE^s_{00} as a function of D, again for $J_z=-0.5$. The spin-flip gap is clearly finite for $D>1$ and $D<-1$; in between these values, however, it extrapolates to a very small value and the scaled mass gap ratio is close to unity. In comparison with the results for $J'_{xy}=0$, the actual gaps are flat over a large range of D. It is exactly this behavior that led the authors of Ref. 18 to question the existence of the Heisenberg singlet phase. If we assume that extrapolation from the available chain lengths gives the correct behavior, then the obtained phase diagram is indeed in agreement, at least topologically, with the phase diagram of the fermion version of the model.

Next we consider another parametrization: we choose $D'=0$ and determine the phase diagram in the $J_zJ'_z$ plane. Taking first the special case $J'_{xy}=0$, the phase diagram estimated from the finite-chain calculations is shown in Fig. 11. By a canonical transformation Hamiltonian (2.2) can be transformed at $J'_{xy}=0$ to a similar Hamiltonian with J'_z replaced by $-J'_z$, and the phase diagram respects this symmetry. The quantum numbers of the eigenstates are changed under this transformation, so the nature of the ground state of the model depends on the sign of J'_z. We find seven different phases, of which 4 are ordered phases and 3 are planar phases, in agreement with the fermion problem whose phase diagram is shown in Fig. 2. For $J_z,J'_z>0$ there is a ferromagnetic phase whose boundary can be determined with a rather good accuracy from the finite-chain calculations. The counterpart of this phase for $J'_z<0$ is a state where the σ_j spins are aligned ferromagnetically, while the τ_j spins are all aligned in the opposite direction.

For $J_z,J'_z<0$ there is an antiferromagnetic ground state. The first excited state in finite chains is symmetric under the interchange of σ_j and τ_j and antisymmetric under time reversal. The gap to this state vanishes exponentially with the chain length. For $J'_z>0$ another antiferromagnetic state is found. Here, however, the first excited state is antisymmetric under the interchange of σ_j and τ_j.

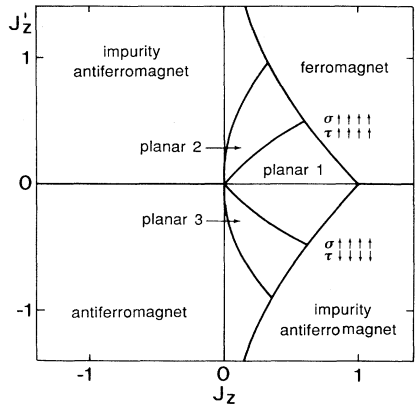

FIG. 11. Phase diagram of the composite-spin model in the $J_zJ'_z$ plane for $D'=0$ and $J'_{xy}=0$.

In the middle of the phase diagram of Fig. 11 we have three planar phases. In the planar 1 phase all the gaps, ΔE_{01}, ΔE_{02}, ΔE^s_{00}, and ΔE^a_{00} vanish as $1/N$. In the planar 2 and planar 3 phases only ΔE^a_{00} vanishes as $1/N$. Extrapolations for locating the boundaries of these phases are very uncertain. To indicate the difficulties in the extrapolation we show in Fig. 12 the scaled mass gap ratios for all four gaps at $J_z=0.2$ as a function of J'_z. To have a simple picture we show the results only for $N=8$ and 10. If the planar 2 and planar 3 phases exist, they do

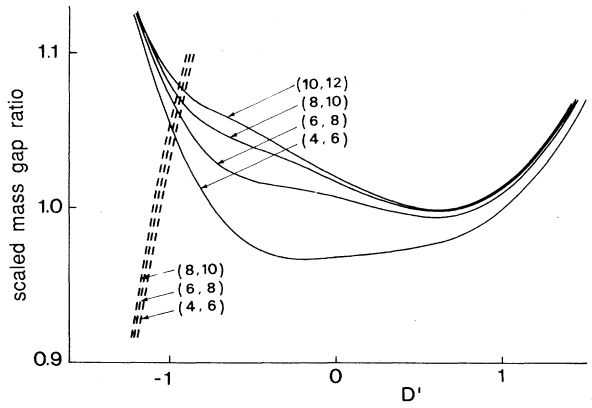

FIG. 10. Scaled mass gap ratios for the gaps ΔE_{01} (solid lines) and ΔE^s_{00} (dashed lines) for $J_z=J'_z=-0.5$ and $J'_{xy}=1$.

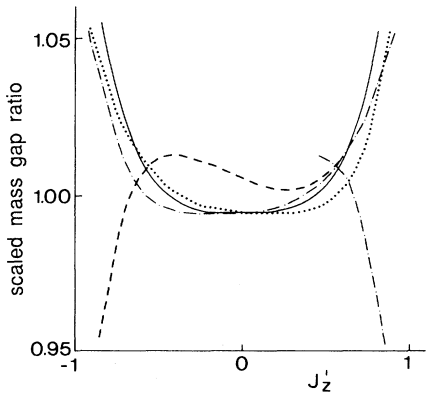

FIG. 12. Scaled mass gap ratios for gaps ΔE_{01} (solid line), ΔE_{02} (dotted line), ΔE^s_{00} (dashed line), and ΔE^a_{00} (dashed-dotted line) vs J'_z for $D'=J'_{xy}=0$ and $J_x=0.2$, comparing chains with 8 and 10 sites.

so in a narrow region only. The antiferromagnetically ordered phase is present for large values of J_z' even for $J_z > 0$, while in the continuum limit model $J_z = 0$ is the phase boundary.

When $J_{xy}' \neq 0$ we would expect that for $J_z < 0$, singlet phases appear on both sides of the $J_z' = 0$ line (cf. Fig. 4). The results for the scaled mass gap ratios at $J_z = -0.5$ are shown in Fig. 13. There is in fact a region near $J_z' \sim -0.5$ where the scaled mass gap ratios are larger than unity for all gaps. For long enough chains this is presumably the case also around $J_z' \sim 0.5$. There is, however, a wide range of J_z' where the scaled mass gap ratio for spin-flip processes is less than unity. The reason for this is that, as was already seen in the case of the other parametrization, the introduction of the J_{xy}' coupling increases the gaps ΔE_{00}^{s} and ΔE_{00}^{a}, but the spin-flip gaps are decreased.

To have an estimate for the phase diagram when $J_{xy}' = 0.2$, we show in Fig. 14 the phase boundaries determined from the condition that the scaled mass-gap ratios calculated for chain lengths of 8 and 10 sites are equal to 1. If we use the same criterion to determine the phase boundaries for varying chain lengths we find that, as the chain length increases, the width of the planar phase decreases, the width of the singlet phase increases, and a second singlet phase will appear. If these tendencies reflect the true asymptotic behavior, we should find for $J_{xy}' = 0.2$ an asymptotic phase diagram similar to the one shown in Fig. 15. This phase diagram is in qualitative agreement with the fermion-gas prediction.

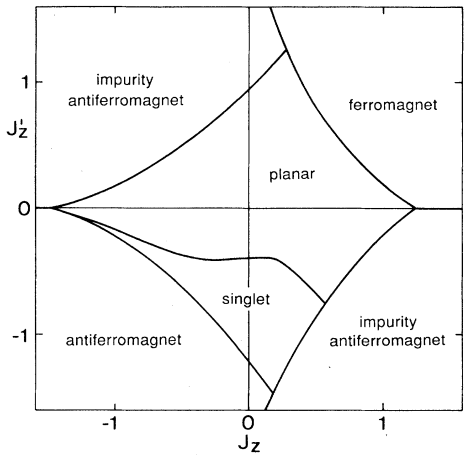

FIG. 14. Phase boundaries in the $J_z J_z'$ plane for $J_{xy}' = 0.2$ determined from the condition that the scaled mass gap ratio for chains with 8 and 10 sites should be equal to unity.

As J_{xy}' tends towards 1 all phase boundaries are shifted but not very much. However, a qualitatively new feature in the phase diagram appears at some value of $J_{xy}' < 1$ which we cannot determine precisely: a *third* singlet

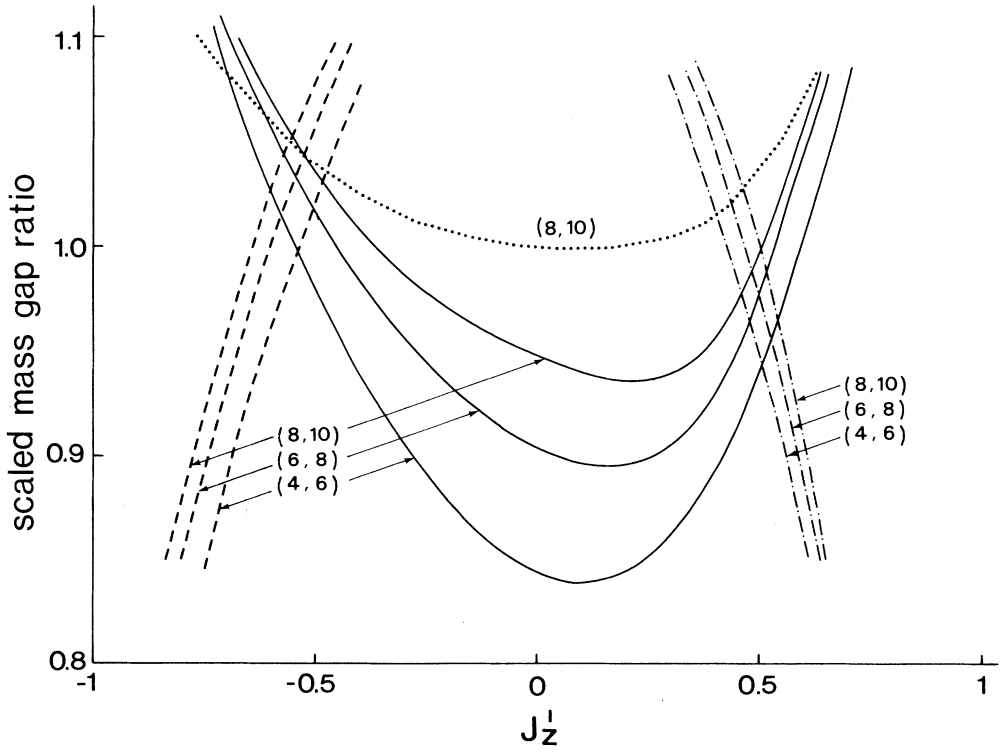

FIG. 13. Scaled mass gap ratios, using the same conventions as in Fig. 12 for $D' = 0$, $J_{xy}' = 0.2$, and $J_z = -0.5$.

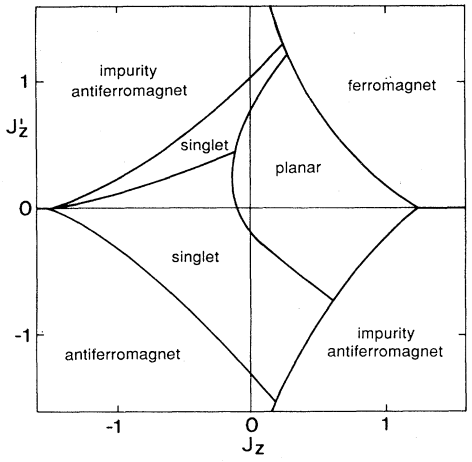

FIG. 15. Phase diagram expected for an infinitely long chain with $J'_{xy}=0.2$.

phase appears between the impurity antiferromagnetic phase and that part of the planar phase which asymptotically becomes the second singlet phase of Fig. 15. As the chain length increases, the planar phase in the $J_z<0$ region is reduced to two narrow "fingers" between the three singlet phases, and if we assume as before that the widths of these fingers are asymptotically zero, we find for $J'_{xy}=1$ an asymptotic phase diagram which is shown in Fig. 16.

Even the topology of the phase diagram of Fig. 16 is different from that of the fermion-model phase diagram shown in Fig. 4. In the fermion picture there is only one line which separates two singlet phases and along which the gap vanishes, while the lattice spin calculation gives two such lines. When $J'_{xy}=1$ the lattice Hamiltonian is

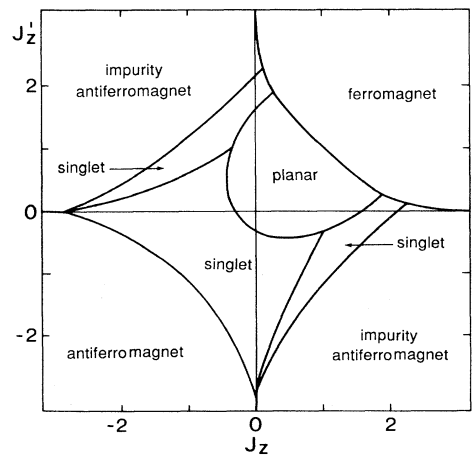

FIG. 16. Phase diagram expected for an infinitely long chain with $J'_{xy}=1$.

symmetric with respect to J_z and J'_z, and the phase diagram of Fig. 15 reflects this symmetry. In the continuum limit J_z and J'_z appear differently in the fermion description and this symmetry is lost. The existence of two singlet phases, suggested by the fermion model in the continuum limit, is incompatible with the symmetries of the original spin model which has either one or three (on present evidence) such phases.

VI. DISCUSSION

We have compared phase diagrams predicted by the fermion representation, and its bosonized version, of a 1D composite-spin model with results from numerical calculations on finite chains. Our aim was to check to what extent the continuum-limit results agree with those obtained on lattices. The composite-spin model considered is the one that has been studied recently[8] in our attempt to see if and how gaps are generated in integer-spin models.[2–4]

To make matters simpler we have chosen two particular parametrizations for the composite-spin model. First we consider the case of finite D' with $J_z=J'_z$, and J'_{xy} is switched on gradually. It is not always easy to deduce the correct infinite-chain length behavior from the available data. It is in fact known[19] for models which are soluble by the Bethe ansatz that the true asymptotic behavior sets in for very long chains. The use of the criterion that the scaled mass gap ratio should be unity at the transition point can lead to incorrect estimates for the phase boundaries. This is in particular the case for Kosterlitz-Thouless–like transitions, where the scaled mass gap ratio should be unity over an extended range of couplings. For this reason the phase boundaries which we have found for the planar phases are not very precise, but they seem to be in qualitative agreement with expectations based on the fermion-model results. There are regions on both sides of the $J_z+D'=0$ line in the phase diagram where the scaled mass gap ratio is larger than unity, although for all gaps by only a few percent. Furthermore these regions grow with increasing chain length. It is conceivable that the spin-flip gap will vanish in the thermodynamic limit along a single line for $J_z<0$, and that singlet phases appear on both sides of this line. If this scenario is true for any finite J'_{xy}, as suggested by Schulz,[7] then the continuum-limit fermion model should give a qualitatively correct description of the properties of the composite-spin model, and hence of the properties of the usual spin-1 Heisenberg model when $J'_{xy}=1$.

The results we find for the second choice of parameters cannot be interpreted as easily, however. We take $D'=0$ and analyze the phase diagram in the $J_zJ'_z$ plane as J'_{xy} is switched on. For small values of J'_{xy} the phase diagram seems to be in agreement with the fermion-model prediction. Using similar arguments as in the previous case, we conclude that as J'_{xy} becomes finite, singlet phases appear on both sides of a line which is close to $J'_z=0$ for $J_z<0$. When $J'_{xy}=1$, these arguments result in three singlet phases, in clear contradiction with the topology of the phase diagram of the fermion model in the continuum limit, which has only two singlet phases. The fermion

model at $J'_{xy}=1$ is in the strong-coupling limit and one could argue that the weak-coupling results do not apply here. We think rather that this discrepancy points to an inherent deficiency of the fermionized (or bosonized) equivalent of the spin problem in the continuum limit. A symmetry which is present in the spin model is lost in the continuum-limit fermion model. Exchanging on every second site the σ_j and τ_j operators, the Hamiltonian (2.4) is transformed such that J_{xy} and J'_{xy}, and J_z and J'_z, are interchanged. Thus the model with $J'_{xy}\neq 0$ and $J_{xy}=0$ has the same phase diagram as the model with $J_{xy}\neq 0$ and $J'_{xy}=0$ if only J_z and J'_z are interchanged. We know from the numerical calculations and from the equivalent extended Hubbard model that no singlet phases exist when $J'_{xy}=0$. Therefore there are no singlet phases when $J_{xy}=0$ and $J'_{xy}\neq 0$, and a finite J_{xy} should only renormalize the velocities of the charge-density and spin-density degrees of freedom without giving rise to relevant operators. This means that it would not be possible to generate singlet phases in the fermion model. This argument is not rigorous, but it shows that the continuum limit can be misleading because of the approximations involved in the course of transforming the original lattice model of Eq. (2.4) into the continuum model of charge-density and spin-density degrees of freedom given by Eqs. (3.17) and (3.18).

Another indication for J'_{xy} not necessarily generating a gap can be obtained from the numerical results. When J'_{xy} becomes finite the gaps ΔE^s_{00} and ΔE^a_{00} are increased, and the phase boundaries of the ordered phases move away from the $D'+J'_z=0$ line. On the other hand the spin-flip gaps ΔE_{01} and ΔE_{02} are decreased together with the related scaled mass gap ratios.

Throughout the analysis reported in this paper we have used argumentation similar to that which finds $D'+J'_z=0$ to be a critical line separating two singlet phases. When this argumentation is applied consistently to the numerical results of the spin-1 model considered here, it seems to result in conflicting interpretations of the data in some parts of the phase space. A convenient explanation to these conflicting results would be the appearance of marginal operators which in short chains would completely mask the true asymptotic behavior. However, in the framework of the present analysis these marginal operators would appear in a rather peculiar way.

As is evident from our results for the behavior of various phase boundaries when the exchange parameters of the model are changed, there is also another possible explanation to the conflicting results which is worth considering. It seems that the charge-density and spin-density degrees of freedom are much more strongly coupled than is generally believed. It is very likely that this coupling, together with the inclusion of renormalization effects, are needed to recover in the fermion language the proper symmetries of the lattice spin model. More work is clearly needed to validate the fermion-gas description of spin models.

---

*Permanent address: Central Research Institute for Physics, H-1525 Budapest, P.O. Box 49, Hungary.

[1]H. E. Lieb and D. C. Mattis, *Mathematical Physics in One Dimension* (Academic, New York, 1966).
[2]F. D. M. Haldane, Phys. Lett. **93A**, 464 (1983); Phys. Rev. Lett. **50**, 1153 (1983).
[3]I. Affleck, Nucl. Phys. B **257**, 397 (1985).
[4]I. Affleck and F. D. M. Haldane, Phys. Rev. B **36**, 5291 (1987).
[5]M. den Nijs, Phys. Rev. B **33**, 611 (1981); Physica **111A**, 237 (1982).
[6]J. Timonen and A. Luther, J. Phys. C **18**, 1439 (1985).
[7]H. J. Schulz, Phys. Rev. B **34**, 6372 (1986).
[8]J. Sólyom and J. Timonen, Phys. Rev. B **34**, 487 (1986); **38**, 6832 (1988).
[9]J. Sólyom, Adv. Phys. **28**, 201 (1979).
[10]H. Shiba, Prog. Theor. Phys. **48**, 2171 (1972).
[11]M. Fowler, J. Phys. C **13**, 1459 (1980).
[12]H. Fukuyama and H. Takayama, in *Electronic Properties of Inorganic Quasi One Dimensional Compounds,* edited by P. Monceau (Reidel, Dordrecht, 1985).
[13]J. E. Hirsch, Phys. Rev. Lett. **53**, 2327 (1984); H. Q. Lin and J. E. Hirsch, Phys. Rev. B **33**, 8155 (1986).
[14]S. Robaszkiwicz, R. Micnas, and K. A. Chao, Phys. Rev. B **23**, 1447 (1981).
[15]B. Fourcade and G. Spronken, Phys. Rev. B **29**, 5089; **29**, 5096 (1984).
[16]R. Botet, R. Jullien, and M. Kolb, Phys. Rev. B **28**, 3914 (1983).
[17]H. J. Schulz and T. A. L. Ziman, Phys. Rev. B **33**, 6545 (1986).
[18]J. Sólyom and T. A. L. Ziman, Phys. Rev. B **30**, 3980 (1984).
[19]F. Woynarowich and H.-P. Eckle, J. Phys. A **20**, L97 (1987).